June 2009 *Volume 5 Issue 3*

Trade Science Inc.

Materials Science

An Indian Journal

Full Paper

MSAIJ, 5(3), 2009 [184-192]

Synthesis and study of micro-structure properties of SiO_2 incorporated polyimide based high temperature resistive nano composite films

D.Shrivastava[1], Anand Kumar Gupta[1, 2]*, J.M.Keller[1, 2], R.Bajpai[2]

[1]Macromolecular Research Centre, R. D. University, Jabalpur-482001, (M.P.), (INDIA)

[2]Department of Post Graduate Studies and Research in Physics and Electronics, R.D. University, Jabalpur-482001, (M.P.), (INDIA)

Tel : +919425389369

E-mail : anandlug2003@yahoo.com

Received: 1st May, 2009 ; Accepted: 6th May, 2009

ABSTRACT

The PI/SiO_2 nano-composite films were prepared using In-situ Generated Nano-Phase Structure (IGNPS) approach from the precursor solution of polyimide (PI) and tetraethoxysilane (TOES). For developing PI/SiO_2 nano-composite films, alkoxysilane which is precursor to tetraethoxysilane (TEOS) was blended with polyamic acid a precursor to PI in an ultra low concentration. FT-IR study was performed to assess the formation of nano-composite films. The silica nano particles were evaluated using AFM technique. Thermal stability of composite films was analyzed using TGA characterization. Microhardness, tensile strength, tensile modulus and elongation were investigated to study the micromechanical performance of nano-composite films. The increase in value of hardness (H_v) and tensile strength for composite films were observed in comparison to pure PI with better thermal stability and low water absorption. The synergistic improvement in PI/TEOS composite films were attribute due to the formation of Si-O-Si particles within the PI matrix. © 2009 Trade Science Inc. - INDIA

KEYWORDS

TOES;
Silica particles;
Thermal stability;
Microhardness;
Micromechanical Properties.

1. INTRODUCTION

Organic-inorganic composites, have been proved as new advanced material because they combine the advantageous properties of organic component e.g. flexibility, low dielectric constant (ε), and processability etc., by previous workers[1-5]. The enhancements in the properties of organic-inorganic hybrids are mainly due to two reasons; (i) The discrete inorganic phases, smaller than100 nm, provide a very large interfacial area between the organic phase and inorganic phase and correspondingly cause the enhancement in the macroscopic properties of hybrids. (ii) Nano-composites having molecular level of dispersion may result in hybrid polymers with specific properties possessing versatile properties especially dielectric, micromechanical and thermal are observed by Matienzo[6]. Polyimide (PI) is being extensively used in microelectronics and aerospace industries. However, PI exhibit relatively high value of water absorption and the coefficient of thermal expansion, which can limit their application in the field of electronics. On the other hand, silica has been considered an ideal separated domain component in hybrids for improving the thermal and mechanical properties of

materials, explained by Schmidt[7]. The combination of nano-scale inorganic moieties with organic polymers has a high potential for future applications and has therefore attracted considerable attention during the recent past. For achieving the best combined properties of PI/inorganic hybrids, improving the compatibility of two phases and reducing the phase separation are critical considerations. In fact, compatibility enhancement is usually generated by an improvement in the interaction between two phases and by a reduction in the size of separated domains. These expectations are usually realized, firstly by the use of reactive polymers and their conversion into PI network matrices; secondly, by the conversion of an inorganic precursor into a network phase, and thirdly by the addition of a coupling agent to enhance the interaction between the inorganic and PI phases. However, because of the difficulty of synthesizing functional PI or PI precursors, the last two routes can only contribute to the effectiveness of the preparation of PI/silica hybrids. The mechanical properties of hybrids obtained with route second usually do not have well enough mechanical properties, while the route third commonly generates larger discrete inorganic domains. In fact, route second is a sol-gel process, in which the silica domain, derived from the hydrolysis of tetraalkoxysilane, is added to PI or its precursor solution, reported by Shindu[8]. From the past decade, the investigated properties of silica/PI nano-composites have mainly been their thermal and mechanical behaviors, explored by Al-kandary[9]. Present study focuses the concept of incorporating ultra low concentration for reduced phase separation and low water sorption with enhanced mechanical and thermal properties, where the hydrolysis and condensation (Polycondensation or self condensation) of TEOS taking place within the PI matrix which is initiated by the water molecules released during thermal imidization of PAA into Polyimide.

Fourier transform infrared spectrometry (FT – IR) is a powerful and potentially very widely used method for obtaining the information about dominance of the chemical functional group of the PI/TEOS nano-composite films. In addition to this, atomic force microscopy (AFM) has been utilized to provide microscopic evidence about the formation of silica particle within the PI matrix. Thermal stability was studied using thermogravimetric analysis (TGA). Microhardness test was performed using Vickers diamond pyramidal indenter attached to Carl Zeiss NU2 universal research microscope and the value of hardness (H_v) was evaluated to obtain information on the structural features and micromechanical property changes for PI/TEOS nano-composite films. Tensile strength, tensile modulus and elongation were studied to obtain information about mechanical properties of prepared PI/TOES nano-composite films.

2. EXPERIMENTAL

2.1. Material and method

Tetraethoxysilane (TEOS) 99% pure was procured from Lancaster, USA and used as silica generating precursor. Polyamic acid (PAA) a condensation product of pyromellitic dianhydride (PMDA) and oxydianiline (ODA) marketed as ABRON S-10 was procured from M/s ABR Organics Ltd., Hyderabad, India (with 11.44% solid content in dimethylacetamide (DMAc) with an inherent viscosity of 1.56 dl/g at 25^0C) and was used as received.

AR grade Tetrahydrofuran (THF), Supplied by Merck was used as co-solvent for the preparation of precursor solution. AR grade methanol, supplied by Merck was used as solvent for the removal of DMAc from the nano-composite films prepared for water sorption analysis.

2.2. Preparation of PI/TEOS blends

The silica generating precursor solutions were prepared by adding TEOS in THF in different calculated compositions i.e. 20% to 10^{-5} wt %. Various concentrations of TEOS were taken in a known volume of THF and added to the calculated quantity of the PAA solution so that films having the ultimate desired concentration of TEOS (i.e. $10^{-5,}$ 10^{-4}, 10^{-3}, 10^{-2}, 10^{-1}, 10 and 20 wt %) could be obtained; these are designated as PS5, PS4, PS3, PS2, PS1, PS10 and PS20, respectively. The unmodified polyimide is designated as PI. The blends were stirred for half an hour in a magnetic stirrer.

2.3. Preparation of PI/TEOS nano-composite films

The blends were weighed over clean and dry glass plates and spread evenly with the help of a glass rod,

Full Paper

so that they resulted in 25 (±0.00002)μ thick films after ultimate curing at 350°C for 2 hrs in air. The cure cycle involved conditioning at 70°C for 24 hours and thereafter, ½ hour each at 100, 150, 200 and 300°C for the first step, which partially imidizes the reactant. Subsequently, these films were heated at 350°C for 2 hrs. Thereafter, the films were allowed to cool slowly to room temperature. The PI film was also cured under identical conditions and designated as PI. The resultant films were of 15 cm^2 in size and 25 ± 0.0002 micron in thickness and used for all the characterizations.

3. Characterizations

3.1. FT-IR

The Fourier Transform Infrared Spectrum (FT-IR) of neat PI, and PI/Silica nano-composites films were characterized using Lambda BX instrument, Perkin Elmer, Singapore.

3.2. AFM

AFM (Atomic Force Microscopy) analysis was performed using Nanoscope III, Digital Instrument, working in contact mode.

3.3. TGA

Dynamic thermogravimetric analysis was performed on a Perkin-Elmer TGA-7 instrument. The heating rate adopted was 10°C/min in an inert atmosphere.

3.4. Water sorption

The water sorption behavior was analyzed using ASTM D570. Samples were dried at 100°C for 1 hr. and dipped in methanol to leach out residual solvent (DMAc). These samples were dried at 120°C for 2 hrs and then dipped in 100 ml of water. The water uptake at different intervals of time till the equilibrium condition were determined by taking the weight of the samples using Perkin-Elmer's Microbalance (Model-AD-4) having accuracy up to 1 microgram.

The water sorption was calculated using equation:

$$\text{Water Uptake (\%)} = [W_0 - W_1 / W_1] \times 100 \quad (1)$$

Where, W_1 is initial weight and W_0 is final weight.

3.5. Microhardness measurement

Microhardness measurements on nano-composite films were carried out using Carl Zeiss NU_2 Universal Research Microscope-mph 160 microhardness tester with a Vickers diamond pyramidal indenter attached to it. The Vickers Hardness Number (H_v) was calculated using equation:

$$H_v = 1.854\ L / d^2, \text{MPa} \quad (2)$$

Where, (L) is load in kg and (d) is diagonal of indentation in mm. For variation of H_v with load, the load was varied from 10 to 100 g.

3.6. Mechanical test

Mechanical strength were carried out on pure PI and PI/TEOS films of size (1×15) cm^2 in length and 25 micron in thickness at room temperature on an Instron Universal Testing Machine (Model No. 4302) according to ASTM test method no. D - 638. The samples were conditioned at 110°C for 24 hours before the testing. The load-elongation curves obtained were converted to stress-strain curves and the following parameters, tensile strength, tensile modulus and elongations, were computed.

4. RESULTS AND DISCUSSION

4.1. FT-IR analysis

FT-IR absorption spectra of the pure PI and PI incorporated TEOS nano-composite films are shown in figure 1. The characteristic absorption spectra of PAA at 1650 cm^{-1} was found to completely disappear, however, the characteristic absorption spectra of the imide unit at 1776, 1777, 1724, 1374 and 722 cm^{-1} wave number were observed for pure PI film and PI/TEOS

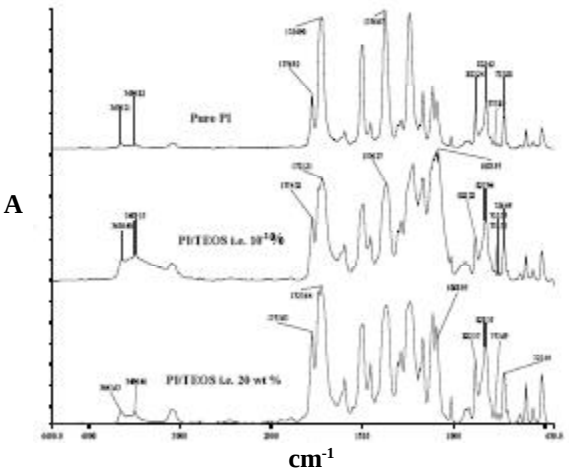

Figure 1: FT-IR spectrum of pure PI, PI/TEOS i.e. 10^{-1} wt % and PI/TEOS i.e. 20 wt % nano-composite films

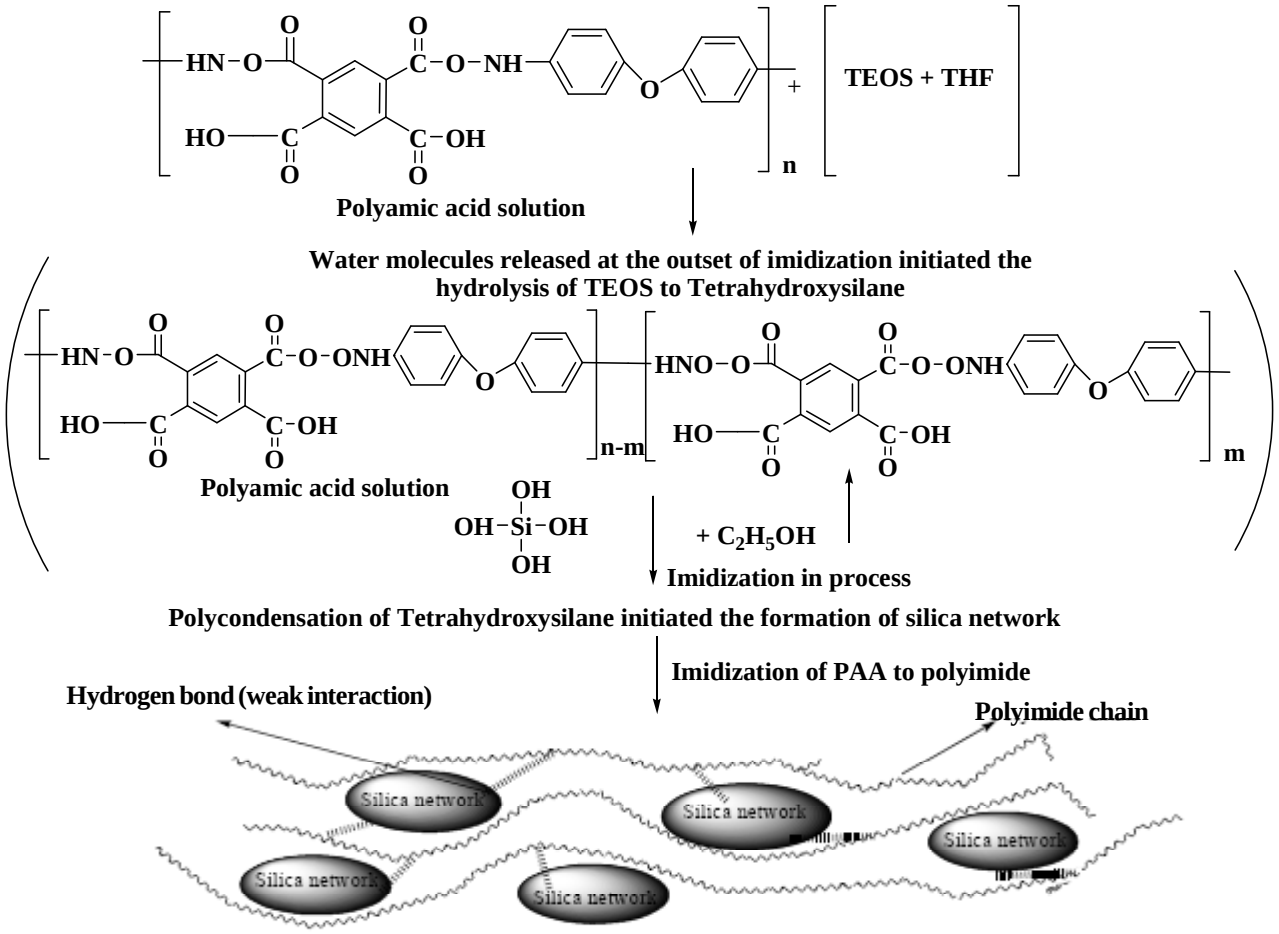

Figure 2: Systematic representation of formation of silica network between the polyimide matrixes when TEOS was incorporated in higher concentration

composite films, reported by Nol[10]. The addition of TEOS did not yield any negative effects on the imidization of PAA. On the other hand, the broad absorption spectrum around 1083 cm-1 was the asymmetric stretching of Si-O-Si units. The absorption intensity of this peak increased with the TEOS concentration. The absorption spectrum at 3400 cm-1 was generated from OH groups. The TEOS incorporated PI nano-composite films in ultra low concentration also show the characteristic absorption spectrum of Si-O-Si unit at 1089 cm^{-1}. This indicates that there are more Si-O-Si bonds in higher concentration. Figure 2 shows the systematic representation of formation of silica network between the polyimide matrixes when TEOS was incorporated in higher concentration. The PI/TEOS (-1%) film shows the particles of much reduced size indicating the formation of less Si-O-Si networks. Figure 3 shows the systematic representation of formation of silica nano particles between the polyimide matrixes when TEOS incorporated in low concentration. Moreover, the absorption bands at 1083 cm^{-1} clearly indicate the efficient conversion of the TEOS in silica within PI matrix.

4.2. AFM analysis

The AFM topographic image of pure PI and PI/TEOS nano-composite films are shown figures 4 to 8. Figure 4 shows the topographic image of neat PI, where a single phase with smooth surface was observed. The topographic image, (Figure 5), clearly revealed that higher concentration containing TEOS films show greater extent of aggregation of silica particles, whereas, ultra low concentration film shows dispersion of silica particles in nano meter regime within PI matrix figures 6 to 8. When concentration of TEOS is relatively higher, the inorganic particles tend to coalesce to form clusters

Full Paper

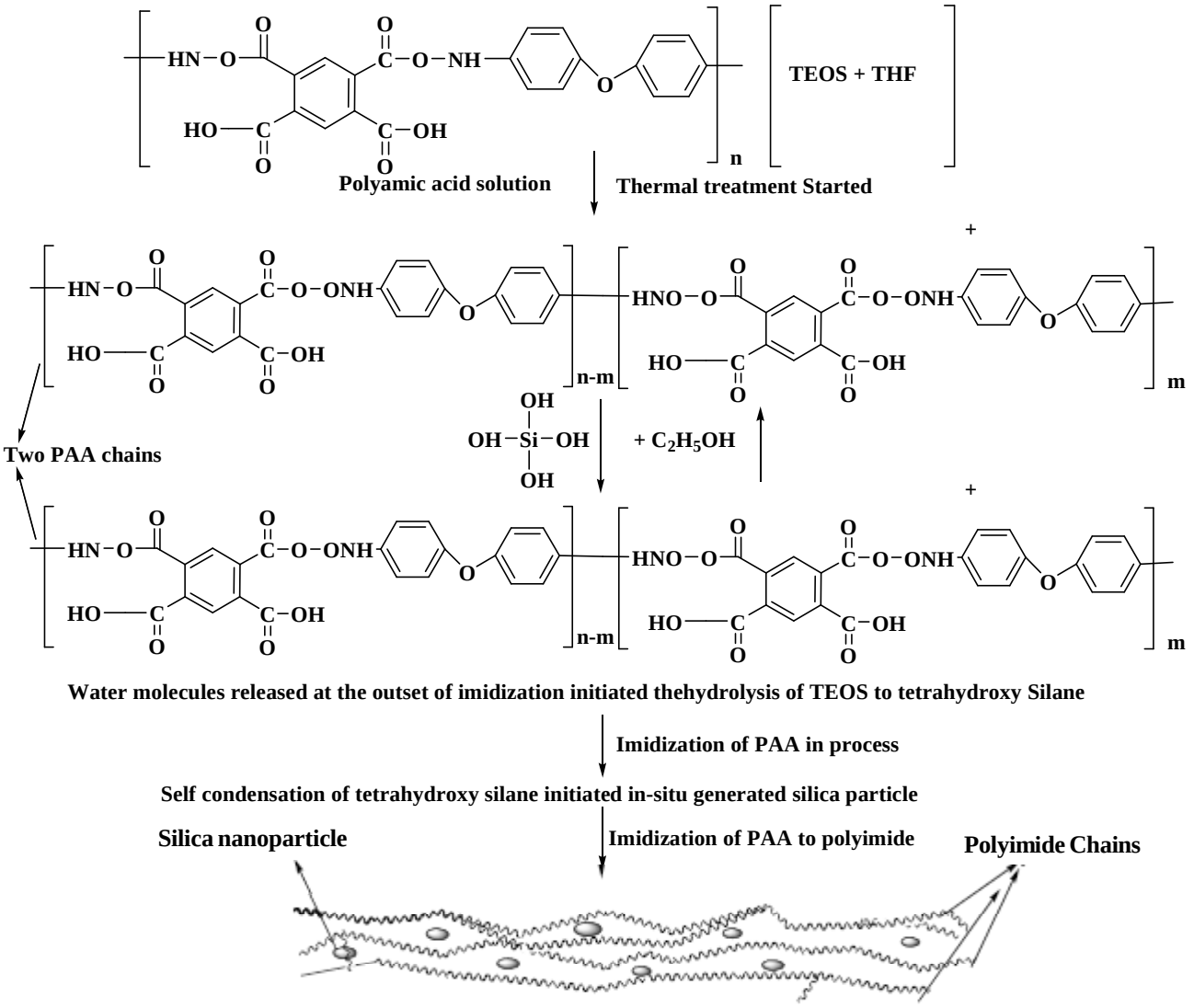

Figure 3 : Systematic representation of formation of silica nano particles between the polyimide matrixes when TEOS was incorporated in ultra low concentration

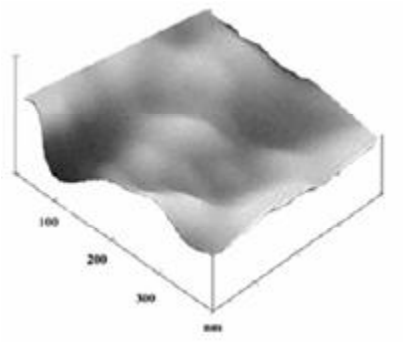

Figure 4: AFM topographic image of neat PI film

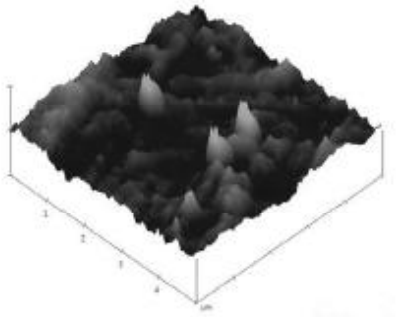

Figure 5 : AFM topographic image of PI/Silica nano-composite film 10^{-4} wt %

of bigger size, approximately of 200-300 nm. However, in the case of ultra low concentration of TEOS, the size of silica particles was reduced up to 80-100 nm with a better dispersion of the particles within the PI

TABLE 1 : Water sorption behaviour of pure PI and PI/TEOS nano-composite films at equilibrium condition

S. no.	Sample designation	Water sorption (%)
1.	Pure PI	2.26
2.	PS20 (20 %)	4.5
3.	PS10 (10 %)	3.45
4.	PS1 (10^{-1} %)	1.59
5.	PS2 (10^{-2} %)	1.56
6.	PS3 (10^{-3} %)	1.73
7.	PS4 (10^{-4} %)	1.54
8.	PS5 (10^{-5} %)	1.48

TABLE 2 : TGA values of pure PI and PI/TEOS nano-composite films

S. no.	Samples	Initial decomposition temperature(IDT)	Residue content at 900°C
1.	Pure PI	517°C	56.77%
2.	PS20 (20 %)	511°C	59.11%
3.	PS10 (10 %)	513°C	57.03%
4.	PS1 (10^{-1} %)	519°C	56.23%
5.	PS2 (10^{-2} %)	527°C	55.14%
6.	PS3 (10^{-3} %)	521°C	56.13%
7.	PS4 (10^{-4} %)	519°C	56.12%
8.	PS5 (10^{-5} %)	516°C	56.01%

matrix. Thus it may be summarized that the incorporation of TEOS in ultra low concentration results in the reduced domain sized in-situ generated silica moiety. This which results in better dispersion as well as improved interfacial interaction of PI chains with the inorganic component within the PI matrix. It has been assumed in the present case that when higher concentrations of silica is used to form the silica network of Si-O-Si type of about 400 to 500 nm approx because in between the matrix TEOS molecules are close by and they tend to initiate the Polycondensation forming network structure Si-O-Si. In case of lower to ultra low concentrations the TEOS molecules are far apart enough and thereby they lead to the self condensation of Tetrahydoxysilane rather than the polycondensation of the tetrahydroxysilane as assumed in case of higher concentrations.

4.3. Water sorption analysis

The water sorption behavior of the PI/TEOS nano-composite films was studied and results are stated in TABLE 1. The water sorption behavior as obtained indicated lower values of water sorption in case of ultra low concentrations of PI/TEOS nano-composite films compared to the value obtained for neat PI. In case of higher concentrations of silica content, such as 20%,

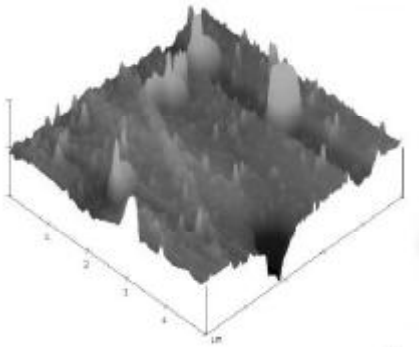

Figure 6 : AFM topographic image of PI/TEOS nano-composite film of 10^{-2} wt %

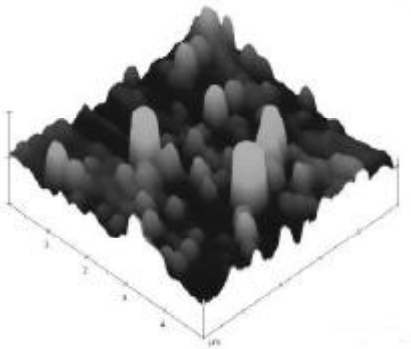

Figure 7 : AFM topographic image of PI/TEOS nano-composite film of 1 wt %

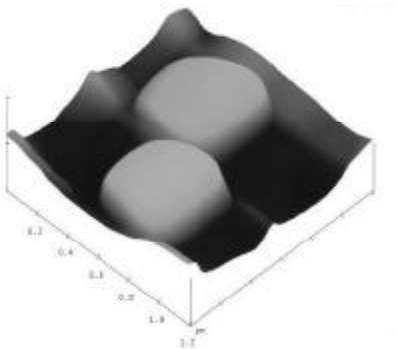

Figure 8 : AFM topographic image of PI/TEOS nano-composite film of 20 wt%.

the value show a steep increase of 4.5% compared to the pure PI value which is 2.26%. While for the case of ultra low concentration the values decreases to 1.48%. This can be explained on the basis of synergistic improvement in the core properties of PI because of smaller compact nanosize silica domain dispersion within the PI matrix which resulted in greater interfacial interaction and dense packing fraction. In each nano-composite film, water uptake was lower than that of neat PI. Lower water sorption in nano-composites may be

Full Paper

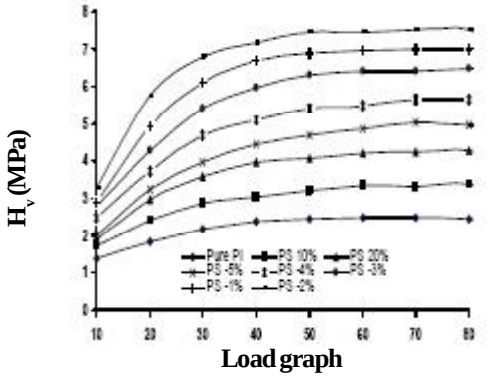

Figure 9 : H_v vs load graph of pure PI and PI/TEOS nano-composite films

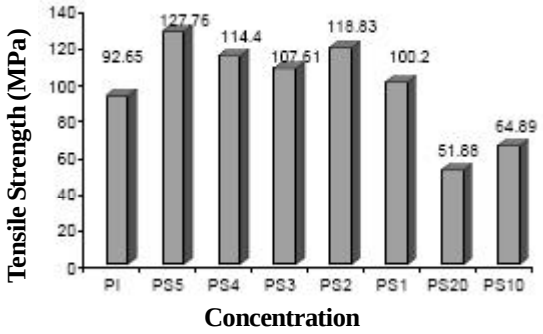

Figure 10 : Bar graph of tensile strength for pure PI and PI/TEOS nano-composite films

attributed to the presence of silica moieties as nano particles in the interstitial sites or in the available free volume of polymeric matrix, thereby filling the free space available for water molecules to reside.

4.4. TGA analysis

TABLE 2 reports the decomposition temperature for neat PI and PI/TEOS nano-composite films. The decomposition temperature of the nano-composite films of higher TEOS content were found to be lower than neat PI, due to elimination of water and C_2H_5OH, which indicate that TEOS was not hydrolyzed completely during the preparation. As the temperature increases imidization of PAA starts and hydrolyzation of TEOS take place alongwith the formation of network. The initial weight loss for the nano-composite films were observed at 517^{0}C, which shows the thermal stability of the nano-composite films. The maximum decomposition temperature of nano-composite films having lower concentration of TEOS shows the favorable reinforcing effect and even dispersion of In-Situ formed silica nano-particles within the PI matrix. The reinforcing effect and even dispersion silica nano-particles limits the segmental motion of the PI chains. The final residue at 900^{o}C is regarded as the real silica content and is proportional to the TEOS concentration suggesting the successful incorporation of silica in PI/SiO_2 nano-composite films.

4.5. Microhardness analysis

The micromechanical aspect of the pure PI and PI/TEOS nano-composite films were studied using microhardness characterization. The microhardness test helps to know that at low loads whether the Vickers hardness number (H_v) is independent, or is dependent, on load. Figure 9 shows the graphical representation of variation between H_v and applied load (L) for pure and nano-composite films. The shape of H_v-load profile trend is almost similar for all specimens. Initially, the microhardness increases with load and thereafter beyond a certain load, (H_v) tends to attain a saturation value. This phenomenon can be explained on the basis of strain hardening in polymers[11,12]. Large scale plastic deformation mainly depends on the micromodes of deformation of polymer chain. This phenomenon happens when sufficient numbers of micromodes become active, as the load is increased, the specimen is subjected to greater strain hardening and H_v is increased, observed by Calleja[13]. When the polymer specimen is fully strain hardened, no appreciable change in the value of H_v will be observed. Thus H_v tends to saturate. TEOS incorporated PI films exhibits higher level of microhardness as compared to pure PI. When TEOS is blended in ultra low concentration, the microhardness increases to a remarkable extent and attains the maximum value.

This increase in microhardness is due to formation of silica nano particles within the PI matrix. However, as the wt% of TEOS increases to 10 to 20 % microhardness tends to decrease as shown in figure 9, however, value of H_v is greater then pure PI film. This decrease in microhardness is due to the silica network to agglomerates into large particles at higher silica loading.

4.6. Strain hardening index

The nature of load dependence of microhardness of the pure and PI/TEOS nano-composite films has been

TABLE 3: Different calculated values of (n) for pure PI and PI/TEOS nano-composite films in the two load regions

S. no.	Samples	Value of (n) for low load regions	Value of (n) for high load regions
1.	Pure PI	2.78	1.56
2.	PS20 (20 %)	2.42	1.78
3.	PS10 (10 %)	2.37	1.82
4.	PS1 (10^{-1} %)	3.13	2.21
5.	PS2 (10^{-2} %)	3.16	2.24
6.	PS3 (10^{-3} %)	3.05	2.08
7.	PS4 (10^{-4} %)	2.99	2.02
8.	PS5 (10^{-5} %)	2.96	1.99

studied using equation (3):

$$L = a.d^n \quad (3)$$

Taking logarithm on both sides of equation (3), we have:

$$\text{Log } L = \log a + n \log d \quad (4)$$

Where (L) is load, (d) is the diameter of indentation, (a) is a constant and (n) is the logarithmic index number, which is the measure of strain hardening. The low load region ranges from 10 to 60 g and high load region ranges from 70 to 100g. The value of (n), for pure PI and nano-composite films are listed in TABLE 3. It is evident that when H_v increases continuously with load, then $n > 2$. The value of (n) approaches a value around 2 in the saturation load region (at which H_v becomes independent of load). Therefore, in low load region (n) is greater than 2. In most of the composite films of ultra low TEOS concentration, the value of (n) is found to be greater then 3 in low load region, and nearly 2 in the high load region.

4.7. Micromechanical analysis

The results of mechanical properties in terms of tensile strength, tensile modulus and elongation of the PI/TEOS nano-composite film are shown from figures 10 to 12. The mechanical properties of a glassy polymeric system depend on the crystallanity introduced into the chains, orientation of the macromolecular segments, and the amount of cross-linking between the macromolecular units. When stress is applied to such materials, the weakest link, i.e., the non-bonded interchain interaction, deforms much easier than the strong covalent bonds along the individual chains. Thus, the network of non-bonded interchain interactions plays a crucial role in determining the magnitude of the strength in that particular polymer. The presence of the crystalline region can lead the polymer to behave like a rigid rod while the amorphous region will compel the polymeric chain to act as an elastomer. The increase in the crystalline region can act as a

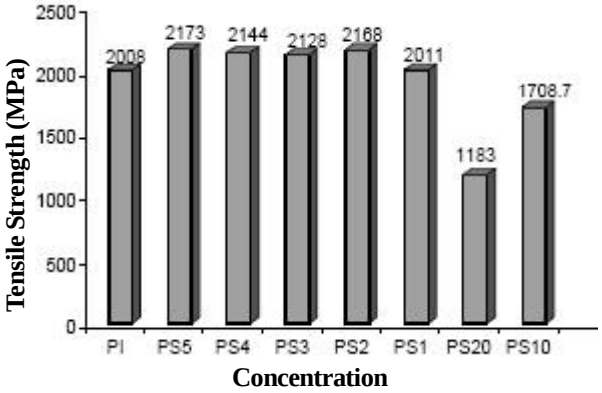

Figure 11 : Bar graph of tensile modulus for pure PI and PI/TEOS nano-composite films

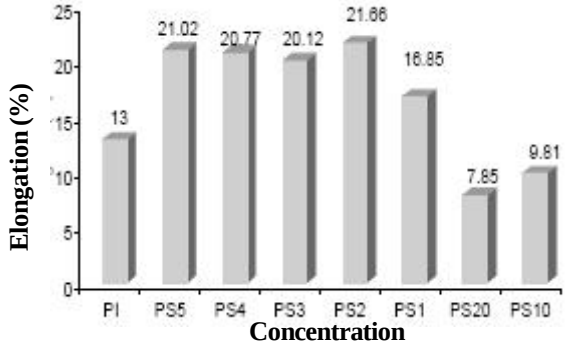

Figure 12 : Bar graph of elongation for pure PI and PI/TEOS nano-composite films

stress raiser and thereby weakens the polymer network to cause premature failure, observed by previous workers[14-16]. It has been observed that, when the TEOS concentrations was less than 10 wt %, both the tensile strength as well as the elongation at break increased in comparison to that of pure PI and as the TEOS content increases to 10 wt % and above, both the tensile strength and the elongation at break was found to be decreased. Nano-composite containing silica nano-domains in ultra low concentration exhibit synergistic improvement in mechanical properties which is due to of two reasons; (a) nanometer-size silica dispersed relatively more homogenously throughout the PI matrix, and (b) PI chains strongly interacted with silica or silanol moieties through hydrogen bonding and consequently became entrapped with silica particles. Silica when introduced in small amount arranges itself in the form of very small particles of nanometer range and thus reinforces the matrix. With the increase in silica content, there is tendency of particle agglomeration, which may result in poor interfacial interactions. The decrease in tensile

strength, tensile modulus and elongation for higher concentration of silica moieties is due to the formation of Si-O-Si networks in the hybrids. In comparison with the PI matrix, the fragile Si-O-Si networks possessed much less tensile strength and poor elongation properties. These properties resulted in intrinsically decreased mechanical performance in the thin nano-composite films, especially in the samples with higher TEOS concentration.

5. CONCLUSION

The new method of preparing PI/TEOS nano-composite films using TEOS as silica precursor has been reported and their relationships to silica contents were investigated. Incorporation of TEOS in ultra low concentration within PI matrix has been proven to be an effective way for preventing phase separation between PI and silica moieties. Controlled incorporation of silica in nano size and its homogenous distribution within PI matrix synergistically enhances the overall performance of prepared nano-composite films. Consequently, the properties of the resultant PI/TEOS thin nano-composite films, such as coefficient of thermal expansion (CTE), thermal decomposition temperature, microhardness, tensile strength, low water sorption behaviour, etc. can be easily manipulated resulting in their effective usage in wide spectrum of applications in nanotechnology.

6. ACKNOWLEDGMENTS

The authors are thankful to SSPL, DRDO for financial support.

7. REFERENCES

[1] K.L.Mittal; 'Polyimide: Synthesis, Characterization & Application', Plenum Press, New-York, **(1984)**.
[2] L.A.Lauis, E.N.Dergacheva, T.J.Zhukova; 'Polyimide: Materials, Chemistry and Characterization', Elsevier Science Pub, USA, **(1989)**.
[3] V.Privallo, T.Shantali, E.Privalko; Polym.Compo., **11**, 63-76 **(2005)**.
[4] J.Liu, Y.Gao, F.Wang, D.Li, J.Xu; J.Mater.Sci., **37**, 3085-3088 **(2002)**.
[5] S.Sasaki, S.Nishi; 'Synthesis of Fluorinated Polyimides: Polyimides, Fundamental and Applications', Marcel Dekker, New-York, **(1996)**.
[6] L.J.Matienzo, F.D.Egitto; J. Mater.Sci., **42**, 239-251 **(2007)**.
[7] H.Schmidt, G.Jonschker, S.Goedick, M.Menning; J. Sol-Jel Sci., **19**, 39-51 **(2000)**.
[8] I.Shindou, S.Katayama, N.Yamada, K.Kamiya; J. Sol-Jel Sci., **30**, 229-237 **(2004)**.
[9] Sh.Al-kandary, A.A.M.Ali, Z.Ahmed; J.Mater. Sci., **41**, 2907-2914 **(2006)**.
[10] W.Nol; 'Chemistry and Technology of Silicones', Academic Press, New-York, **(1968)**.
[11] S.F.Bartram; 'Hand book of X-Ray Diffraction', McGraw, New-York, **(1961)**.
[12] W.Mason, P.F.Johnson, J.R.Warner; J.Mater.Sci., **26**, 6576-6580 **(1991)**.
[13] F.J.B.Calleja, D.S.Sanditov, V.P.Privalko; J.Mate. Sci., **37**, 4507-4516 **(2002)**.
[14] D.R.Paul, S.Newman; 'Polymer Blends', Academic Press, New-York, **(1978)**.
[15] R.A.Fava; 'Methods of Experimental Physics Polymer Part B: Crystal Structure and Morphology', Academic Press, NewYork, **(1980)**.
[16] G.Zamfirova, V.Lorenzo, R.Benavente, J.M.Perena; J.Appl.Polym.Sci., **88**, 1974-1798 **(2003)**.